

TULIP: TOKEN-LENGTH UPGRADED CLIP

Anonymous authors

Paper under double-blind review

ABSTRACT

We address the challenge of representing long captions in vision-language models, such as CLIP. By design these models are limited by fixed, absolute positional encodings, restricting inputs to a maximum of 77 tokens and hindering performance on tasks requiring longer descriptions. Although recent work has attempted to overcome this limit, their proposed approaches struggle to model token relationships over longer distances and simply extend to a fixed new token length. Instead, we propose a generalizable method, named TULIP, able to upgrade the token length to any length for CLIP-like models. We do so by improving the architecture with relative position encodings, followed by a training procedure that (i) distills the original CLIP text encoder into an encoder with relative position encodings and (ii) enhances the model for aligning longer captions with images. By effectively encoding captions longer than the default 77 tokens, our model outperforms baselines on cross-modal tasks such as retrieval and text-to-image generation.

1 INTRODUCTION

Obtaining text representations for long captions in vision-language models is an open research challenge. Within the context of text-only large language models, this problem has been studied extensively (Chung et al., 2024; Touvron et al., 2023; Bai et al., 2023; Gu & Dao, 2023; Su et al., 2024; Dubey et al., 2024; Pawar et al., 2024; Jiang et al., 2024; Lieber et al., 2024), yet, methods for context length expansion have only scarcely made their way into the vision-language domain. For instance, contrastive vision-language models like CLIP (Radford et al., 2021; Jia et al., 2021; Li et al., 2022) are constrained to short input sequences, capped at 77 tokens. Natively, such models based on Transformers (Vaswani et al., 2017) process their input as an unordered set of tokens and use positional encoding to preserve order information (Yun et al., 2019). In particular, CLIP models use absolute positional encodings, which rely on a predefined maximum number of tokens, thereby limiting the input sequence to 77 tokens by design. We introduce an efficient and generalizable method, TULIP, that upgrades the context window size of CLIP-like models.

Recently, Long-CLIP (Zhang et al., 2024) highlighted this problem and proposed an approach for unlocking the long-text capabilities of CLIP. However, their approach focuses on stretching the existing absolute positional encodings, which primarily addresses the issue of the hard token limit but it continues to rely on absolute encodings which inhibit the model’s comprehension of pairwise token relationships. To address the challenge of comprehensively modeling the pairwise distances between tokens, more flexible positional encoding methods have been proposed (Shaw et al., 2018; Su et al., 2024; Golovneva et al., 2024). For example, relative positional encodings offer an approach that allows the model to capture interactions between tokens more effectively, regardless of their placement in the sequence (Su et al., 2024). While this method has shown promise in natural language processing tasks, it remains unexplored in vision-language models. This is not surprising, as extending the context length in vision-language models by switching to more flexible positional encodings is computationally costly because of its significant retraining efforts.

Our proposed method upgrades the context window size of CLIP-like models by utilizing relative positional encodings, which are not restricted to a fixed length. Changing the model in this manner normally requires expensive multi-modal retraining. Instead, we propose an adaptation phase to first distill the knowledge of the original CLIP into the new model with relative positional encodings using only caption data. Such a distillation approach is flexible and can be applied to CLIP-like models constrained by the standard 77-token window, transforming it into a model capable of han-

dling longer captions. Afterwards, we perform full fine-tuning on the distilled model for a single epoch on 1 million image-caption pairs (Chen et al., 2023b), to further improve the alignment between images and long captions. After these phases, our TULIP model can ingest captions longer than the usual 77 tokens and we observe improved performance on tasks ranging from cross-modal retrieval to text-to-image generation, compared to (interpolated) fixed token-window baselines.

In addition to our new method, we introduce a new benchmark for long captions adapted from the recently introduced Dense Captioning Images (DCI) dataset (Urbanek et al., 2024). This benchmark overcomes the limitations of existing retrieval benchmarks which lack diversity, as they focus on specific scenes (e.g., Urban-1K (Zhang et al., 2024)), or are in-distribution datasets with already saturated performance (e.g., ShareGPT4v test set (Chen et al., 2023b)). Our results show that evaluating in a true long caption setting is crucial for evaluating contrastive vision-language mode as they unearth an increased performance gap as compared to prior benchmarks.

In summary, our contributions are: (1) We propose TULIP, the first contrastive vision-language model with relative positional encoding for long captions. (2) We propose a general training procedure to adapt the positional encoding of CLIP-like models using a two-step adaptation encompassing relative position distillation and expansion. (3) We demonstrate improved performance across different cross-modal retrieval and image generation tasks. We introduce a new benchmark Long-DCI for a more comprehensive evaluation of long-caption retrieval tasks.

2 RELATED WORK

Position Encodings in Transformer Models. Transformers, the foundational architecture for many vision-language models, rely on positional encodings to compensate for the lack of inherent positional awareness in their set-based representation. In the natural language domain, absolute positional encodings (Vaswani et al., 2017) were initially proposed, where fixed embeddings are added to token embeddings based on their position in the sentence sequence. However, as models have grown larger and more complex, alternative approaches emerged such as relative positional encodings (Shaw et al., 2018; Press et al., 2021), randomized positional encodings (Ruoss et al., 2023), extrapolation techniques (Press et al., 2022) and positional interpolation (Chen et al., 2023c). Other works, such as Rotary Position Embedding (RoPE) (Su et al., 2024) and its variations (Chen et al., 2023c; Peng et al., 2023), apply relative positional encodings without any modifications to the self-attention mechanism, making it computationally efficient. Another recent approach is Contextual Position Encodings (CoPE) (Golovneva et al., 2024), which is a more general position encoding technique enabling one to attend to the i -th particular word, noun, or even sentence. In contrastive vision-language models, integrating positional information effectively across modalities remains an unsolved challenge and this is the primary focus of this paper.

Contrastive Vision-Language Models with Long Captions. Contrastive Vision-language models have made significant strides in aligning visual and textual modalities, driven by the success of large-scale pre-trained models such as CLIP (Radford et al., 2021), ALIGN (Jia et al., 2021), BLIP (Li et al., 2022) and many others (Garg et al., 2023; Vasu et al., 2024b;a; Cherti et al., 2023; Sun et al., 2023). These models leverage contrastive learning techniques to align image and text representations in a shared feature space, enabling robust performance on tasks such as image-text retrieval and zero-shot classification. However, all these models focus on short, global textual descriptions, often limited by small context windows, such as the 77-token limit in CLIP. Recent research has started considering this limitation, for instance, DCI (Urbanek et al., 2024) highlights the problem by pointing out that CLIP’s 77-token limit restricts the model from accommodating detailed, dense captions. DreamLIP (Zheng et al., 2024) studies the usage of synthetically generated long captions under the contrastive learning framework but uses subsampled short captions from longer captions instead of processing the complete long captions. Long-CLIP (Zhang et al., 2024) engages the challenge more directly, by stretching absolute position encodings through interpolation to enable fine-tuning on long captions. However, interpolation only partially addresses the limitations of absolute encodings when processing longer, complex captions. This is because interpolation merely extends the existing positional information without fundamentally altering its nature or capabilities. These limitations include diminished ability to capture fine-grained relative positions and poor generalization to longer captions (Pawar et al., 2024). We propose an alternative approach that incorporates relative encodings without training from scratch, thereby enabling more effective processing of long captions and the comprehension of the pairwise token relationships therein.

3 TULIP

In this section, we introduce our method Token-Length Upgraded CLIP (TULIP). We start by stating the problem setting, followed by introducing the positional encoding swapping and the two-step adaptation procedure: (i) relative position distillation and (ii) relative position expansion.

3.1 PROBLEM STATEMENT

Let model f be a contrastive vision-language model, such as CLIP, designed to align text and images in a shared embedding space. The text encoder of f , denoted as f_T is constrained to processing sequences up to a predefined number of 77 tokens, denoted by $T_f = 77$. This is due to the fixed absolute positional encodings $P_f \in \mathbb{R}^{77 \times d}$, where d is the dimensionality of the embeddings. Given an input sequence $x = [x_1, x_2, \dots, x_n]$, where $n > T_f$, the model truncates x to $x' = [x_1, \dots, x_{T_f}]$ losing critical information from the sequence beyond the first 77 tokens.

Our objective is to transform model f into model g , without any re-training from scratch, to enable processing sequences of arbitrary length T_g . In this new model g , the token-length constraint of f_T is removed, allowing the model to handle inputs of length $T_g > 77$.

3.2 POSITIONAL ENCODING SWAPPING

In f_T , the positional encoding function $P_f(i)$ maps each token position i to a vector in \mathbb{R}^d , within a window of size 77. To overcome this limitation, we redefine the positional encoding function for model g , denoted as $P_g(i)$ which scales with input length T_g . This new function allows the model g to process captions of arbitrary length without truncation.

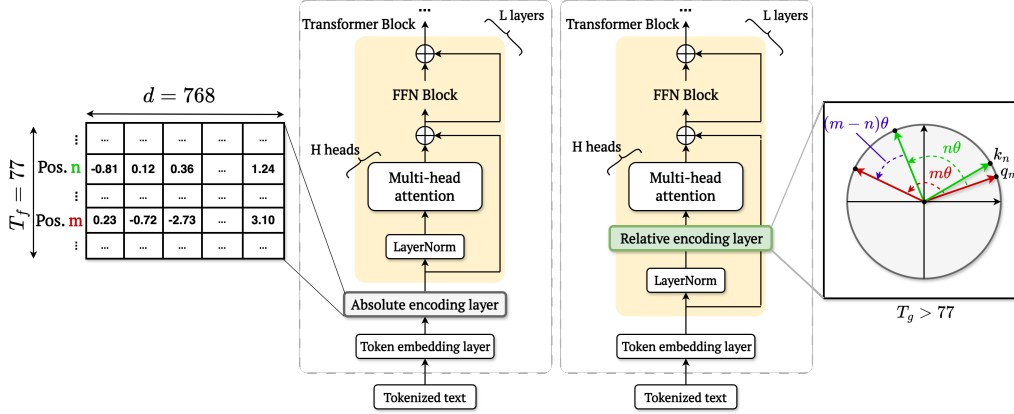


Figure 1: **Swapping the Positional Encoding.** We update CLIP models by replacing the absolute positional encoding with relative positional encoding in each transformer block. This modification allows for long caption understanding and better modeling of pairwise token dependencies.

We implement $P_g(i)$ as Rotary Positional encodings (RoPE) (Su et al., 2024) presented in Figure 1. Unlike traditional absolute positional encodings, where each position in a sequence is assigned a fixed vector, RoPE rotates the embeddings based on the relative distance between tokens. More specifically, we alter the calculation of the attention weights within the self-attention layers of the text encoder f_T , which are initially calculated as $\text{softmax}(\frac{q_m^T k_n}{\sqrt{d}})$, where:

$$q_m = W_q x_m, k_n = W_k x_n, \quad (1)$$

representing the query and key vectors respectively for the m -th and n -th tokens in the sequence x , and W_q, W_k are their learned projection matrices. With RoPE, we inject the position information of each token x_i into the q_m and k_n vectors by:

$$q_m = R_{\Theta, m} W_q x_m, \quad k_n = R_{\Theta, n} W_k x_n, \quad (2)$$

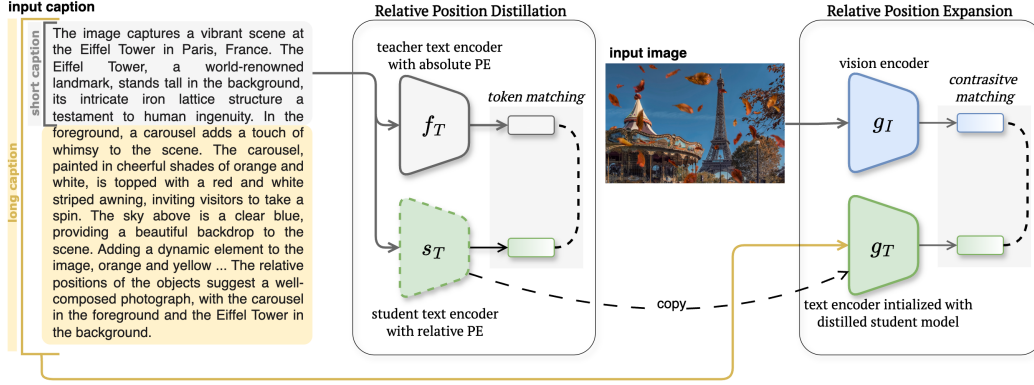


Figure 2: **TULIP training procedure.** First, we perform relative position adaptation by distilling the knowledge of the CLIP text encoder into a student text encoder initialized with relative position encodings. This stage uses the first 77 tokens of a long caption (the gray block). The second stage is the relative position expansion, where we fine-tune the distilled text encoder with captions longer than 77 tokens (the combined gray and yellow blocks), together with the vision encoder.

where $R_{\Theta, m}$ and $R_{\Theta, n}$ represent rotation matrices and Θ is the rotational frequency associated with the j -th dimension of the embedding. The rotational frequency ensures that different dimensions of the token embeddings rotate differently, embedding both absolute and relative positional information into the self-attention mechanism.

3.3 RELATIVE POSITION DISTILLATION

Once the architectural changes are in place, the next challenge is to adapt the text encoder of model g to handle both short and long text inputs while retaining the image-text alignment capabilities of model f . We achieve this through knowledge distillation, shown with the first block of Figure 2, where f_T acts as the teacher and the text encoder with the new relative encodings as the student s_T . A key advantage of this approach is that it eliminates the need to retrain the model from scratch despite the introduction of new relative positional encodings. Instead, we distill the knowledge from f_T , transferring its capabilities to the student model without losing the original alignment performance. This method is not only efficient but also generalizable, making it applicable to any text encoder that requires adaptation to new positional encodings.

Let $x = [x_1, x_2, \dots, x_n]$ represent an input caption, where $n \leq T_f$. Both the teacher model f_T and the student model s_T encode this sentence into a shared embedding space. Specifically, the teacher model f_T aggregates the sequence into a special text token and yields the output embeddings $z_{f_T} = f_T(x)$. Similarly, the student model yields output embeddings $z_{s_T} = s_T(x)$. The distillation loss is formulated as a cosine similarity between z_{f_T} and z_{s_T} , aiming to maximize their alignment:

$$\mathcal{L}_{\text{distill}} = \frac{z_{f_T} \cdot z_{s_T}}{\|z_{f_T}\| \|z_{s_T}\|}. \quad (3)$$

This loss function ensures that the student model s_T learns from the teacher model f_T , by leveraging the original model’s ability to align textual and visual information. After the distillation, the student model s_T has the capabilities of the teacher model for encoding up to 77 tokens with relative positional encodings. The only missing feature is the ability to process longer context which is addressed next.

3.4 RELATIVE POSITION EXPANSION

Finally, we expand the context length of model g beyond the original 77-token limit by fine-tuning it with longer captions, shown in the second block of Figure 2. We start by copying the student model weights into the text encoder of g . This is followed by employing Neural Tangent Kernel (NTK)-aware scaled RoPE (bloc97, 2023), a refined version that adapts to the changing length of the input. In particular, we aim to scale the rotational frequency Θ by a factor $(\alpha * \frac{T_a}{T_f}) - (\alpha - 1)$,

where α is a hyperparameter, to accommodate the training of the new higher token positions. The objective behind such scaling is to resolve the problem of losing high-frequency information when interpolating the RoPE embeddings to the higher token positions. In model g , the new positional encodings now support input sentences x_g of arbitrary length, $T_g > T_f$. We proceed with fine-tuning using the usual contrastive loss as follows: $\mathcal{L}(x, y) = -\log \frac{\exp(\cos(z_x, z_y)/\tau)}{\sum_{y'} \exp(\cos(z_x, z_{y'})/\tau)}$, where x is the sentence, y is the image and τ is the temperature hyperparameter. However, to keep the original capability for handling short sentences as well, we jointly optimize two contrastive loss terms for both long and short sentences, as follows:

$$\mathcal{L}_{\text{total}}(x_{T_g}, x_{T_f}, y) = \lambda \times \mathcal{L}_{\text{short}}(x_{T_f}, y) + (1 - \lambda) \times \mathcal{L}_{\text{long}}(x_{T_g}, y). \quad (4)$$

The first loss term, $\mathcal{L}_{\text{short}}$, is designed to preserve the model’s ability to handle short captions, aligning with the capabilities of model f . The other term, $\mathcal{L}_{\text{long}}$, is introduced to ensure that model g can process longer captions effectively.

By extending the context length in this manner, model g becomes capable of handling both short and long captions, making it more versatile for a wide range of vision-language tasks as we will demonstrate in the experiments.

4 EXPERIMENTS & RESULTS

Datasets and downstream tasks. We evaluate TULIP on three downstream tasks: short caption cross-modal retrieval, long caption cross-modal retrieval, and text-to-image generation. For short caption cross-modal retrieval, we follow Zhang et al. (2024) and evaluate our model on the COCO2017 5k validation set (Lin et al., 2014) and the full Flickr30k dataset (Plummer et al., 2015). Similarly, for long caption cross-modal retrieval, we use two datasets namely ShareGPT4V test split and Urban-1K. Both datasets contain 1,000 image-caption pairs, collected by Zhang et al. (2024) and recaptioned using the ShareGPT4V captioning model.

It is important to recognize that long-caption cross-modal retrieval benchmarks come with several limitations. These include a lack of diversity, as some focus on narrowly defined scenes (e.g., Urban-1K), while others consist of in-distribution datasets where performance is already saturated (e.g., ShareGPT4V). To overcome these challenges, we introduce a new benchmark for long captions adapted from the recently introduced Dense Captioning Images (DCI) dataset (Urbanek et al., 2024). **Long-DCI** includes 7,000 human-annotated images and *long* caption pairs, with captions averaging 200 tokens per image. This human-led annotation process ensures diverse and accurate descriptions, avoiding the biases inherent in AI-generated captions like those from ShareGPT4V.

Evaluation metrics. We report image-to-text and text-to-image retrieval performance using recall as the standard evaluation metric. Our evaluation process is the same for all experiments, including how we handle long input tokens. For each dataset, we choose the best design and settings using a validation set, and then report the final results on the test set.

		Long-DCI		ShareGPT4V		Urban-1K	
		Img2Txt	Txt2Img	Img2Txt	Txt2Img	Img2Txt	Txt2Img
ViT-B-16	CLIP	35.9	33.7	78.2	79.6	68.1	53.6
	Fine-tuned CLIP	46.3	45.4	94.1	93.6	80.4	79.8
	Long-CLIP	42.1	48.4	94.6	93.3	78.9	79.5
	TULIP (Ours)	50.2	50.6	98.6	98.6	88.1	86.6
ViT-L-14	CLIP	35.0	37.0	81.8	84.0	68.7	52.8
	Fine-tuned CLIP	51.6	50.7	95.3	95.4	78.0	76.5
	Long-CLIP	54.0	46.1	95.8	95.6	82.7	86.1
	TULIP (Ours)	55.7	56.4	99.0	99.0	90.1	91.1

Table 1: **Long caption cross-modal retrieval comparison** on Long-DCI, ShareGPT4V and Urban-1K. TULIP consistently outperforms other CLIP variants across all evaluated datasets and tasks. Note that we adopt the results for CLIP and Long-CLIP from Zhang et al. (2024), while we fine-tune CLIP (Fine-tuned CLIP) on ShareGPT4V ourselves.

		COCO				Flickr30k			
		Img2Txt		Txt2Img		Img2Txt		Txt2Img	
		R@1	R@5	R@1	R@5	R@1	R@5	R@1	R@5
ViT-B-16	CLIP	51.8	76.8	32.7	57.7	44.1	68.2	24.7	45.1
	Fine-tuned CLIP	37.4	62.3	21.8	43.4	25.7	45.8	17.9	34.5
	Long-CLIP	57.6	81.1	40.4	65.8	46.8	71.4	34.1	56.3
	TULIP (Ours)	56.8	80.3	40.7	66.1	46.1	70.8	35.2	57.4
ViT-L-14	CLIP	56.1	79.5	35.4	60.1	48.5	72.6	28.0	49.3
	Fine-tuned CLIP	37.9	63.1	23.1	45.1	26.0	46.3	17.9	34.9
	Long-CLIP	62.8	85.1	46.3	70.8	53.4	77.5	41.2	64.1
	TULIP (Ours)	62.6	84.7	46.1	71.1	56.7	79.5	41.6	64.3

Table 2: **Short caption cross-modal retrieval comparison on COCO and Flickr30k.** TULIP shows competitive performance, often matching or exceeding Long-CLIP across different metrics and backbones.

Training details. Our training procedure comprises two phases: relative position distillation and relative position expansion, both utilize the ShareGPT4V dataset (Chen et al., 2023b) containing 1M image and long caption pairs. During the relative position distillation phase, we truncate captions to the first 77 tokens for both the teacher and student models. We train the student model using cosine loss as the distillation loss function for 20 epochs with a batch size of 640 using the AdamW optimizer (Loshchilov, 2017), setting the learning rate to 5e-4 with 1000 warmup steps. In the relative position expansion phase, we employ full-length captions without truncation, exposing the model to comprehensive-textual details. The full TULIP model, featuring the new distilled text encoder, is fine-tuned using the NTK approach, with α empirically set to 8.0. For all main experiments, we use 248 number of tokens to match Long-CLIP’s context length for a fair comparison. Note that we can increase the length to more tokens, as shown in our ablations. We perform this fine-tuning stage for a single epoch with a batch size of 1280, a learning rate of 1e-5, and 1000 warmup steps using AdamW. We base our implementations on OpenAI’s pre-trained CLIP-ViT-B-16 and CLIP-ViT-L-14 architectures (Ilharco et al., 2021). Our code will be made publicly available.

4.1 CROSS-MODAL RETRIEVAL COMPARISON

We evaluate TULIP against the original CLIP, fine-tuned CLIP on ShareGPT4V (Chen et al., 2023b), and Long-CLIP Zhang et al. (2024) for both long-caption (Table 1) and short-caption (Table 2) cross-modal retrieval tasks. As shown in Table 1, our proposed model outperforms all benchmarks in long-caption cross-modal retrieval across 3 datasets on both image-to-text and text-to-image retrieval, utilizing two different vision backbones: ViT-B-16 and ViT-L-14 (Dosovitskiy et al., 2021). On the Long-DCI dataset, which is a more challenging benchmark for all approaches, we can observe that Long-CLIP already shows improvement over the original CLIP and that our TULIP model further improves on this. These results demonstrate the efficacy of TULIP in enhancing CLIP’s capabilities for long-caption cross-modal retrieval, particularly in diverse scenarios. For short captions, as shown in Table 2, we find that the tailored approach used by Long-CLIP for the first 20 tokens is beneficial for the short caption performance as they outperform CLIP even on short captions. Whereas TULIP is able to obtain competitive performance without needing to specifically tailor to the first 20 tokens, which demonstrates the flexibility of relative positional encodings across different caption lengths. Overall, the results in Table 1 and 2 indicate that TULIP is effective not only for long captions but also for maintaining competitive performance in short caption retrieval scenarios.

4.2 TEXT-TO-IMAGE GENERATION

In this section, we evaluate qualitatively how our proposed procedure enhances text-to-image generation by simply replacing the original CLIP ViT-L-14 text encoder with our TULIP model, in particular using the text encoder. We use Stable Diffusion XL (SDXL) (Podell et al., 2023) as the image generation backbone. Note that do not perform any additional training of the diffusion model. As observed in Figure 3, TULIP demonstrates improvements in both long and short caption under-

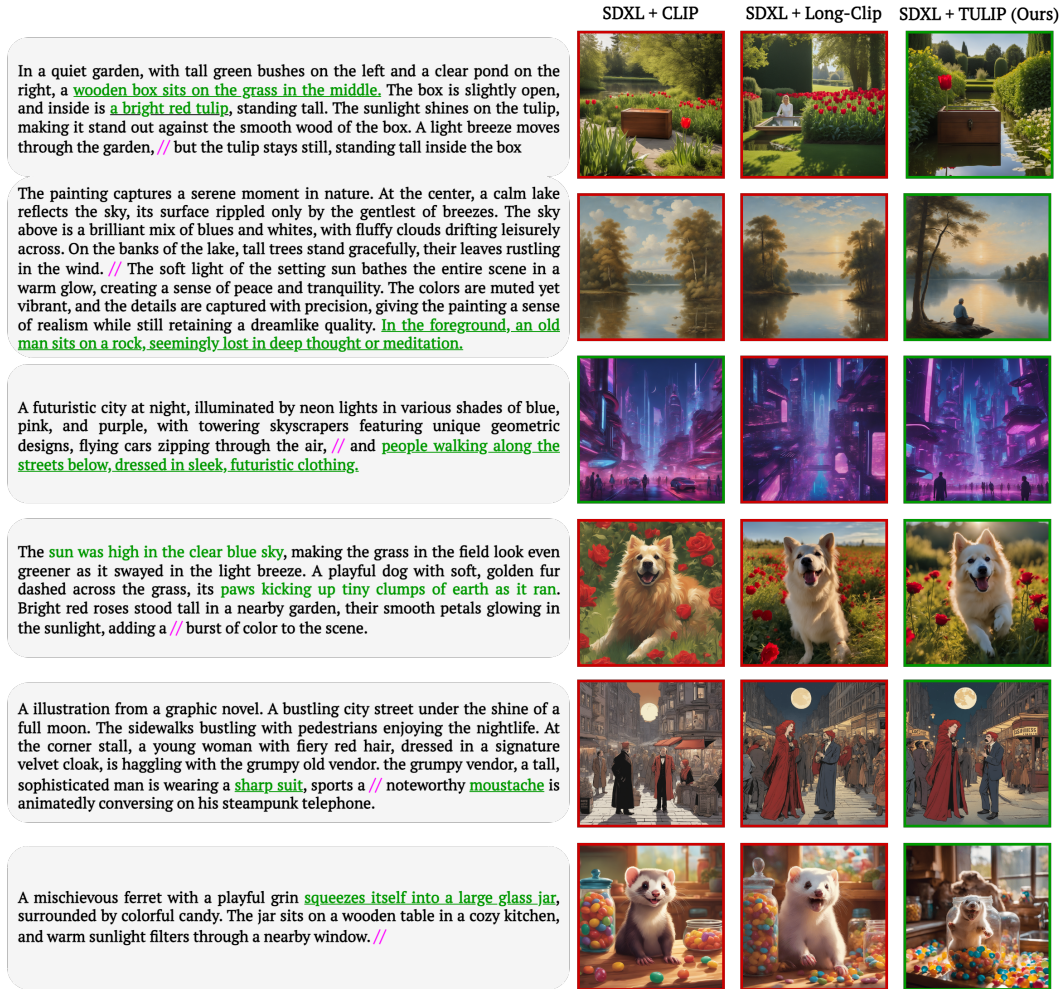


Figure 3: **Text-to-Image Generation results.** We replace the text encoder of SDXL with our own TULIP model. We observe improvements in both long captions understanding and capturing nuanced details, compared to the baselines CLIP-ViT-L-14 and Long-CLIP. Note that the // marks the 77-token boundary in the caption. The words in green indicate visual concepts that are correctly generated by TULIP and are missed by the baselines.

standing and modeling of nuanced details. For example, our version of SDXL + TULIP accurately depicts “the red tulip inside a wooden box” in the first example. This is not the case with SDXL-CLIP or SDXL-Long-CLIP which generate many tulips in the garden, missing the key detail of a single tulip being inside the box. This observation shows that our model can indeed capture finer details in the description. The second example shows that our model successfully generates “an old man sits on a rock” even when this detail appears beyond the 77-token limit. On the other hand, both base CLIP and Long-CLIP encoders fail at this. A similar observation is in the third example where the model correctly captures “people walking along the streets”. These examples are direct evidence that our approach can truly capture the meaning of words in longer captions. For shorter prompts, our model also shows enhanced caption understanding. For instance, it accurately represents the ferret with a “playful grin” demonstrating the enhanced association of attributes with their corresponding nouns. Even more impressively, it accurately places the ferret inside a “large glass jar”, showing correct spatial understanding - something both CLIP and Long-CLIP fail to achieve. These observations suggest that our TULIP text encoder enhances long caption comprehension, resulting in more accurate and contextually rich image generation across varying prompt lengths. We provide additional results in the appendix.

Positional encodings	Long-DCI		ShareGPT4V		Urban-1K	
	Img2Txt	Txt2Img	Img2Txt	Txt2Img	Img2Txt	Txt2Img
CoPE	50.8	49.9	98.5	97.8	86.7	82.8
RoPE	55.7	56.4	99.0	99.0	90.1	91.1

Table 3: **Ablation comparing different relative position encodings: RoPE and CoPE in TULIP.** RoPE generalizes better across varying or extended sentence lengths, especially on out-of-distribution datasets, namely Long-DCI and Urban-1k.

4.3 ABLATION STUDY

In this section, we carefully analyze various design choices for our proposed method. We examine different positional encoding schemes, investigate the impact of context length, and explore variations in the distillation loss function.

Different types of Relative Positional Encodings In this experiment, we compare different types of relative positional encodings. We choose a recently introduced Contextual Position Encoding (CoPE) (Golovneva et al., 2024) for implementing the relative positional encodings in the text encoder. Afterwards, we perform the distillation and context length extension phases using the same dataset and parameters as with RoPE (Su et al., 2024). In Table 3 we observe that RoPE outperforms CoPE in long-caption retrieval tasks. This is due to RoPE’s strong ability to generalize across varying or extended sentence lengths, even beyond those on which the model was originally trained. In contrast, CoPE struggles to generalize as effectively when sequence lengths increase, as its embeddings are more dependent on the specific context within which they were trained. This explains why CoPE performs similarly to RoPE on the ShareGPT4V test split (same training distribution), but shows a larger performance gap on the Long-DCI and Urban-1k datasets.

The impact of the caption length. Next, we evaluate the impact of varying context lengths on the performance of RoPE in long-caption image retrieval tasks. To investigate this, we fine-tune only the text encoder during the context length extension phase with different context sizes (which are $n \times 77$): $\{77, 154, 231, 308\}$ tokens while keeping the image encoder frozen. We deliberately freeze the image encoder to isolate the text encoder’s performance, as unfreezing it could potentially mask the text encoder’s limitations in processing longer inputs. Figure 4 presents the model’s performance across three datasets (ShareGPT4V, Urban-1K, and Long-DCI) for cross-modal retrieval tasks. We observe general improvement in performance with increased context length, particularly from 77 to 154 tokens, across all datasets. This improvement is more pronounced for image-to-text retrieval, suggesting that longer contexts enhance text representation and enable more precise alignment with image features. However, we observe a slight performance plateau or minor decline for 308-length sentences, signaling a point of diminishing returns where additional tokens may introduce noise or redundancy. This plateau is likely due to the average caption length in our training data being 174.02 tokens, explaining why performance levels off between 154 and 231 tokens.

Benefit of using cosine distillation loss. In this section, we vary the distillation loss function used during the relative position adaptation phase and report the results in Table 4. As seen, the cosine loss performs better than other alternatives across different datasets and tasks. We believe this is attributed to its alignment with the normalized embedding space of CLIP models and its scale invariance property. The scale invariance of cosine loss proves particularly beneficial in this distillation setup, where the student model (ViT-L-14 with the added RoPE or CoPE layer) can produce embeddings with different magnitudes compared to the teacher model. This invariance allows the distillation process to focus on transferring the essential directional information of the embeddings, rather than being influenced by potential scale discrepancies introduced by the RoPE or CoPE layer. As a result, cosine loss consistently outperforms other loss functions like L2 and MSE across various datasets (Long-DCI, ShareGPT4V, Urban-1K) and cross-modal tasks such as image-to-text and text-to-image, demonstrating its effectiveness in preserving the semantic relationships learned by the teacher model.

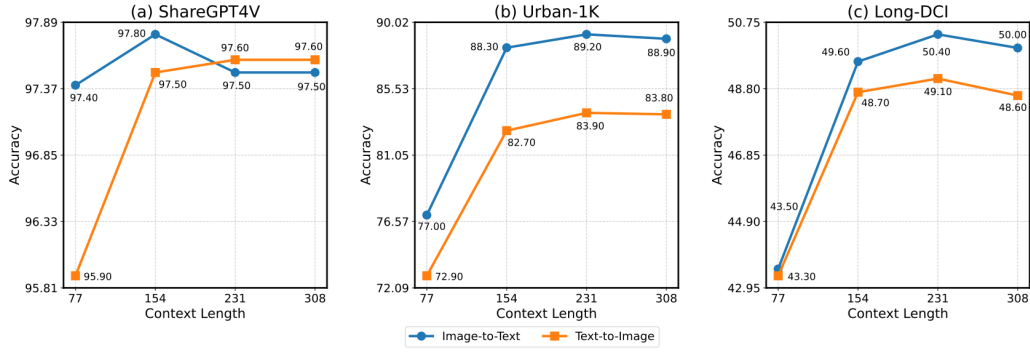


Figure 4: **Impact of the sequence length on cross-modal retrieval tasks.** We observe general improvement in performance with increased sequence length, particularly from 77 to 154 tokens, across all datasets and tasks.

Distillation loss	Long-DCI		ShareGPT4V		Urban-1K	
	Img2Txt	Txt2Img	Img2Txt	Txt2Img	Img2Txt	Txt2Img
CLIP	35.0	37.0	81.8	84.0	68.7	52.8
L2	39.4	35.8	84.8	83.9	70.2	56.3
MSE	36.4	31.8	83.0	81.3	74.0	53.9
Cosine	38.5	35.8	84.8	84.2	73.6	56.6

Table 4: **Ablation comparing different distillation loss terms in TULIP.** Cosine loss yields the best performance across different datasets and tasks.

4.4 ADDITIONAL ANALYSIS

Attention spread visualization. The effectiveness of our model in long cross-modal retrieval tasks and image generation is largely due to its distinct attention distribution patterns. To illustrate this, we visualize the attention scores between the CLS text token and its preceding tokens in the final attention block of the text encoder, as shown in Figure 5. For comparison, we provided attention visualizations for both our TULIP and LongCLIP. This analysis reveals two key advantages of our model when processing a 248-token caption. First, our model exhibits a more uniform distribution of attention across input tokens, demonstrating its ability to expand the attention scope and effectively aggregate information from a broader range of tokens. This expanded attention field improves the model’s performance in long-caption tasks by capturing and utilizing details from later parts of the caption that other models might overlook. Second, our model shows increased attention to punctuation symbols, particularly commas, which enhances its ability to parse and segment longer texts. Such capability is crucial for better comprehension of complex, multi-caption descriptions.

Caption-image relevance distribution analysis. This analysis investigates where relevant information is distributed within long captions given an image. The aim is to highlight how useful content is spread throughout the whole caption. We analyze 100 randomly selected images with long captions from the ShareGPT4V dataset. For each image-caption pair, we computed the visual embeddings of the image and compared them to the text embeddings of the caption subwindow. We define sliding subwindows of sizes 20, 33, and 55 tokens, moving from left to right with strides of 5, 10, and 15 tokens respectively. We then calculated the cosine similarity between the image encoding and the text encodings of each subwindow, visualized in Figure 6. The figure shows that the similarity scores are distributed across different subwindows, emphasizing the need for models capable of processing longer input sequences. Notably, as window size increases, the similarity patterns become more concentrated and pronounced, suggesting that larger context windows capture more cohesive and relevant information. Additionally, the variability in similarity across different windows highlights the non-uniform distribution of image-relevant information throughout the captions. This reinforces the need to leverage the entire textual sequence when learning image-text representations.

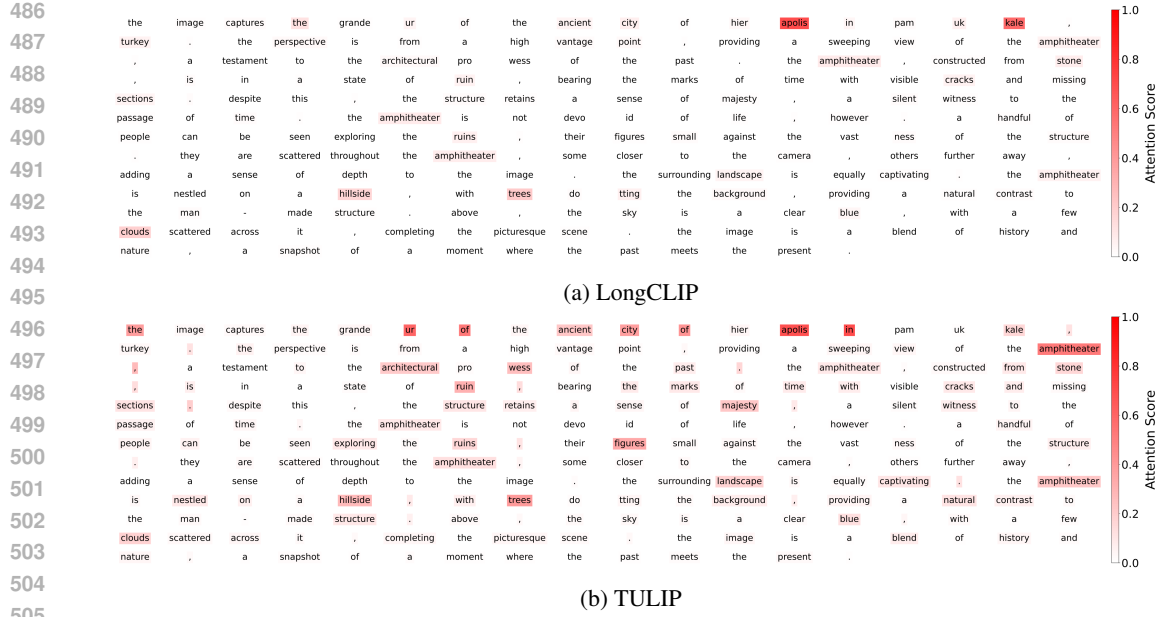


Figure 5: **Attention Spread Visualization** comparing (a) LongClip and (b) TULIP. Our model achieves uniform attention across tokens, demonstrating superior capabilities in parsing and segmenting longer texts with precision.

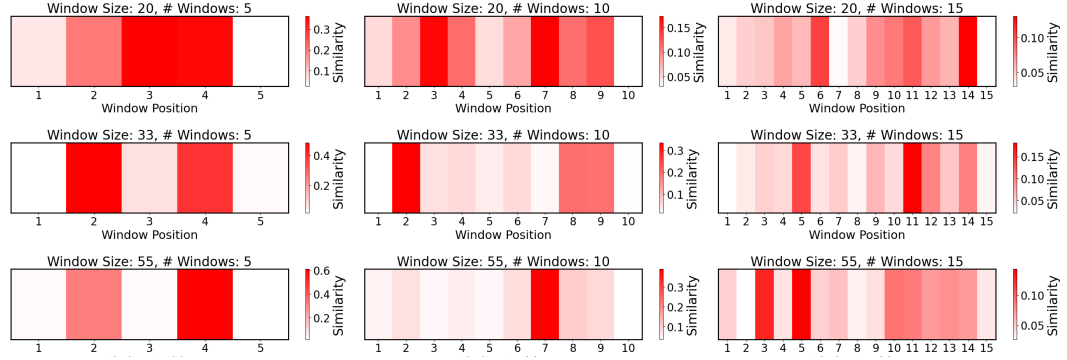


Figure 6: **Caption-image relevance distribution analysis** across varying window sizes and positions. it shows that image-relevant information is spread throughout captions, emphasizing the need for models to process longer text inputs to capture all pertinent details.

5 CONCLUSION

In this work, we addressed the limitations of CLIP-like models in handling long input sequences. We introduce TULIP, a generalizable method that upgrades the context length beyond the 77-token limit. By leveraging relative positional encodings, our approach enables the effective modeling of pairwise token relationships. Through a two-step training process, we successfully adapt the CLIP-like model to process longer captions without compromising its performance on shorter inputs. Our experiments demonstrate that TULIP considerably improves long-caption performance on cross-modal tasks such as retrieval and text-to-image generation, setting a new standard for vision-language contrastive models that require handling complex, extended text descriptions.

Limitations. Our reliance on ShareGPT4V dataset, synthesized by GPT4V (Achiam et al., 2023), limits TULIP’s performance to the quality of GPT4V’s long captions. Furthermore, while TULIP is theoretically capable of handling longer contexts due to the nature of the relative positional encodings, its token length is constrained by the average token length of the ShareGPT4V captions.

REFERENCES

- Josh Achiam, Steven Adler, Sandhini Agarwal, Lama Ahmad, Ilge Akkaya, Florencia Leoni Aleman, Diogo Almeida, Janko Altenschmidt, Sam Altman, Shyamal Anadkat, et al. Gpt-4 technical report. *arXiv preprint arXiv:2303.08774*, 2023.
- Jinze Bai, Shuai Bai, Yunfei Chu, Zeyu Cui, Kai Dang, Xiaodong Deng, Yang Fan, Wenbin Ge, Yu Han, Fei Huang, et al. Qwen technical report. *arXiv preprint arXiv:2309.16609*, 2023.
- bloc97. NTK-Aware Scaled RoPE allows LLaMA models to have extended (8k+) context size without any fine-tuning and minimal perplexity degradation. https://www.reddit.com/r/LocalLLaMA/comments/141z7j5/ntkaware_scaled_rope_allows_llama_models_to_have/, 2023.
- Junsong Chen, Jincheng Yu, Chongjian Ge, Lewei Yao, Enze Xie, Yue Wu, Zhongdao Wang, James Kwok, Ping Luo, Huchuan Lu, et al. Pixart-
- \
- alpha : *Fasttrainingofdiffusiontransformerforphotorealistictext – to – imagesynthesis*. *arXiv preprint arXiv:2310.00426*, 2023a.
- Lin Chen, Jisong Li, Xiaoyi Dong, Pan Zhang, Conghui He, Jiaqi Wang, Feng Zhao, and Dahua Lin. Sharegpt4v: Improving large multi-modal models with better captions. *arXiv preprint arXiv:2311.12793*, 2023b.
- Shouyuan Chen, Sherman Wong, Liangjian Chen, and Yuandong Tian. Extending context window of large language models via positional interpolation. *arXiv preprint arXiv:2306.15595*, 2023c.
- Mehdi Cherti, Romain Beaumont, Ross Wightman, Mitchell Wortsman, Gabriel Ilharco, Cade Gordon, Christoph Schuhmann, Ludwig Schmidt, and Jenia Jitsev. Reproducible scaling laws for contrastive language-image learning. In *Proceedings of the IEEE/CVF Conference on Computer Vision and Pattern Recognition*, 2023.
- Hyung Won Chung, Le Hou, Shayne Longpre, Barret Zoph, Yi Tay, William Fedus, Yunxuan Li, Xuezhi Wang, Mostafa Dehghani, Siddhartha Brahma, et al. Scaling instruction-finetuned language models. *Journal of Machine Learning Research*, 2024.
- Alexey Dosovitskiy, Lucas Beyer, Alexander Kolesnikov, Dirk Weissenborn, Xiaohua Zhai, Thomas Unterthiner, Mostafa Dehghani, Matthias Minderer, Georg Heigold, Sylvain Gelly, Jakob Uszkoreit, and Neil Houlsby. An image is worth 16x16 words: Transformers for image recognition at scale, 2021.
- Abhimanyu Dubey, Abhinav Jauhri, Abhinav Pandey, Abhishek Kadian, Ahmad Al-Dahle, Aiesha Letman, Akhil Mathur, Alan Schelten, Amy Yang, Angela Fan, et al. The llama 3 herd of models. *arXiv preprint arXiv:2407.21783*, 2024.
- Saurabh Garg, Mehrdad Farajtabar, Hadi Pouransari, Raviteja Vemulapalli, Sachin Mehta, Oncel Tuzel, Vaishaal Shankar, and Fartash Faghri. Tic-clip: Continual training of clip models. *arXiv preprint arXiv:2310.16226*, 2023.
- Olga Golovneva, Tianlu Wang, Jason Weston, and Sainbayar Sukhbaatar. Contextual position encoding: Learning to count what’s important. *arXiv preprint arXiv:2405.18719*, 2024.
- Albert Gu and Tri Dao. Mamba: Linear-time sequence modeling with selective state spaces. *arXiv preprint arXiv:2312.00752*, 2023.
- Xiwei Hu, Rui Wang, Yixiao Fang, Bin Fu, Pei Cheng, and Gang Yu. Ella: Equip diffusion models with llm for enhanced semantic alignment. *arXiv preprint arXiv:2403.05135*, 2024.
- Gabriel Ilharco, Mitchell Wortsman, Ross Wightman, Cade Gordon, Nicholas Carlini, Rohan Taori, Achal Dave, Vaishaal Shankar, Hongseok Namkoong, John Miller, Hannaneh Hajishirzi, Ali Farhadi, and Ludwig Schmidt. Openclip, July 2021. URL <https://doi.org/10.5281/zenodo.5143773>. If you use this software, please cite it as below.

- Chao Jia, Yinfei Yang, Ye Xia, Yi-Ting Chen, Zarana Parekh, Hieu Pham, Quoc Le, Yun-Hsuan Sung, Zhen Li, and Tom Duerig. Scaling up visual and vision-language representation learning with noisy text supervision. In *International Conference on Machine Learning*, 2021.
- Albert Q Jiang, Alexandre Sablayrolles, Antoine Roux, Arthur Mensch, Blanche Savary, Chris Bamford, Devendra Singh Chaplot, Diego de las Casas, Emma Bou Hanna, Florian Bressand, et al. Mixtral of experts. *arXiv preprint arXiv:2401.04088*, 2024.
- Junnan Li, Dongxu Li, Caiming Xiong, and Steven Hoi. Blip: Bootstrapping language-image pre-training for unified vision-language understanding and generation. In *International Conference on Machine Learning*, 2022.
- Opher Lieber, Barak Lenz, Hofit Bata, Gal Cohen, Jhonathan Osin, Itay Dalmedigos, Erez Safahi, Shaked Meirom, Yonatan Belinkov, Shai Shalev-Shwartz, et al. Jamba: A hybrid transformer-mamba language model. *arXiv preprint arXiv:2403.19887*, 2024.
- Tsung-Yi Lin, Michael Maire, Serge Belongie, James Hays, Pietro Perona, Deva Ramanan, Piotr Dollár, and C Lawrence Zitnick. Microsoft coco: Common objects in context. In *European Conference on Computer Vision*, 2014.
- I Loshchilov. Decoupled weight decay regularization. *arXiv preprint arXiv:1711.05101*, 2017.
- Saurav Pawar, SM Tonmoy, SM Zaman, Vinija Jain, Aman Chadha, and Amitava Das. The what, why, and how of context length extension techniques in large language models—a detailed survey. *arXiv preprint arXiv:2401.07872*, 2024.
- Bowen Peng, Jeffrey Quesnelle, Honglu Fan, and Enrico Shippole. Yarn: Efficient context window extension of large language models. *arXiv preprint arXiv:2309.00071*, 2023.
- Bryan A Plummer, Liwei Wang, Chris M Cervantes, Juan C Caicedo, Julia Hockenmaier, and Svetlana Lazebnik. Flickr30k entities: Collecting region-to-phrase correspondences for richer image-to-sentence models. In *IEEE International Conference on Computer Vision*, 2015.
- Dustin Podell, Zion English, Kyle Lacey, A. Blattmann, Tim Dockhorn, Jonas Muller, Joe Penna, and Robin Rombach. Sdxl: Improving latent diffusion models for high-resolution image synthesis. *ArXiv*, abs/2307.01952, 2023.
- Ofir Press, Noah A Smith, and Mike Lewis. Train short, test long: Attention with linear biases enables input length extrapolation. *arXiv preprint arXiv:2108.12409*, 2021.
- Ofir Press, Noah Smith, and Mike Lewis. Train short, test long: Attention with linear biases enables input length extrapolation. In *International Conference on Learning Representations*, 2022.
- Alec Radford, Jong Wook Kim, Chris Hallacy, Aditya Ramesh, Gabriel Goh, Sandhini Agarwal, Girish Sastry, Amanda Askell, Pamela Mishkin, Jack Clark, et al. Learning transferable visual models from natural language supervision. In *International conference on machine learning*, pp. 8748–8763. PMLR, 2021.
- Adam Roberts, Colin Raffel, Katherine Lee, Michael Matena, Noam Shazeer, Peter J Liu, Sharan Narang, Wei Li, and Yanqi Zhou. Exploring the limits of transfer learning with a unified text-to-text transformer. *Google, Technical Report*, 2019.
- Anian Ruoss, Grégoire Delétang, Tim Genewein, Jordi Grau-Moya, Róbert Csordás, Mehdi Bannani, Shane Legg, and Joel Veness. Randomized positional encodings boost length generalization of transformers. *arXiv preprint arXiv:2305.16843*, 2023.
- Peter Shaw, Jakob Uszkoreit, and Ashish Vaswani. Self-attention with relative position representations. *arXiv preprint arXiv:1803.02155*, 2018.
- Jianlin Su, Murtadha Ahmed, Yu Lu, Shengfeng Pan, Wen Bo, and Yunfeng Liu. Roformer: Enhanced transformer with rotary position embedding. *Neurocomputing*, 568:127063, 2024.
- Quan Sun, Yuxin Fang, Ledell Wu, Xinlong Wang, and Yue Cao. Eva-clip: Improved training techniques for clip at scale. *arXiv preprint arXiv:2303.15389*, 2023.

- Hugo Touvron, Louis Martin, Kevin Stone, Peter Albert, Amjad Almahairi, Yasmine Babaei, Nikolay Bashlykov, Soumya Batra, Prajjwal Bhargava, Shruti Bhosale, et al. Llama 2: Open foundation and fine-tuned chat models. *arXiv preprint arXiv:2307.09288*, 2023.
- Jack Urbanek, Florian Bordes, Pietro Astolfi, Mary Williamson, Vasu Sharma, and Adriana Romero-Soriano. A picture is worth more than 77 text tokens: Evaluating clip-style models on dense captions. In *Conference on Computer Vision and Pattern Recognition*, 2024.
- Pavan Kumar Anasosalu Vasu, Hadi Pouransari, Fartash Faghri, and Oncel Tuzel. Clip with quality captions: A strong pretraining for vision tasks. *arXiv preprint arXiv:2405.08911*, 2024a.
- Pavan Kumar Anasosalu Vasu, Hadi Pouransari, Fartash Faghri, Raviteja Vemulapalli, and Oncel Tuzel. Mobileclip: Fast image-text models through multi-modal reinforced training. In *Conference on Computer Vision and Pattern Recognition*, 2024b.
- Ashish Vaswani, Noam Shazeer, Niki Parmar, Jakob Uszkoreit, Llion Jones, Aidan N Gomez, Łukasz Kaiser, and Illia Polosukhin. Attention is all you need. *Advances in Neural Information Processing Systems*, 2017.
- Chulhee Yun, Srinadh Bhojanapalli, Ankit Singh Rawat, Sashank J Reddi, and Sanjiv Kumar. Are transformers universal approximators of sequence-to-sequence functions? *arXiv preprint arXiv:1912.10077*, 2019.
- Beichen Zhang, Pan Zhang, Xiaoyi Dong, Yuhang Zang, and Jiaqi Wang. Long-CLIP: Unlocking the long-text capability of clip. *arXiv preprint arXiv:2403.15378*, 2024.
- Kecheng Zheng, Yifei Zhang, Wei Wu, Fan Lu, Shuailei Ma, Xin Jin, Wei Chen, and Yujun Shen. Dreamlip: Language-image pre-training with long captions. In *European Conference on Computer Vision*, 2024.

A APPENDIX

A.1 ADDITIONAL TEXT-TO-IMAGE GENERATION RESULTS



A wide landscape at sunset, with towering mountains in the background, their peaks capped with snow, while in the foreground, a dense forest of pine trees covers the rolling hills, and a serene river flows through, reflecting the pink and orange hues of the sky, with scattered birds flying in the distance.



An old library room filled with wooden shelves, stacked with ancient leather-bound books, their spines worn with age, while a grand chandelier hangs from the ceiling, casting warm light over the room, with a spiral staircase leading up to a balcony that overlooks the lower level of the library.



A medieval marketplace in the town square, bustling with activity, where vendors sell goods from wooden carts, displaying fresh fruits, vegetables, and handmade crafts, while townsfolk dressed in period clothing gather around, conversing and haggling over prices, with the grand castle in the background towering over the scene.

Figure 7: Text-to-Image Generation results.



An enchanted forest at dawn, where glowing mushrooms light up the forest floor, trees with twisted trunks and sparkling leaves reach towards the sky, and magical creatures like fairies and wisps float through the air, while a waterfall cascades into a crystal-clear pond in the background.



A peaceful rural village nestled in the hills, where stone cottages with thatched roofs are surrounded by vibrant gardens, and narrow cobblestone streets wind through the village, leading to a small church with a tall steeple in the center of town, as farmers and villagers go about their daily activities.



A grand cathedral at sunset, its towering spires casting long shadows over the cobblestone plaza, where people gather to admire the intricate stained-glass windows that glow in the fading light, and inside, the grand organ and high vaulted ceilings create an atmosphere of awe and reverence.

Figure 8: **Text-to-Image Generation results.**

A.2 HUMAN EVALUATION OF IMAGE GENERATION

We design a pilot human evaluation by manually crafting captions and generating images by using Stable Diffusion XL (SDXL) with CLIP and TULIP-based text encoders. The resulting images are randomized, and annotators are tasked with selecting the image that is best aligned with the prompt (See Figure 14). They were instructed to evaluate alignment based on objects, their attributes, and their relationships. A total of 15 annotators reviewed 20 samples. We report the results in Table 5.



A serene beach at dawn, where the waves gently lap against the shore, the sand soft and golden underfoot, and palm trees sway in the light breeze, while seagulls call overhead and a lone sailboat drifts on the horizon as the sun rises, casting a golden light across the water.



A rainy, bustling city street at night, where neon signs in vibrant colors reflect off the wet pavement, people with umbrellas hurry along the sidewalks, and taxis drive past, while towering skyscrapers loom overhead, and steam rises from the grates in the street, adding to the moody atmosphere.



An ancient temple in the jungle, overgrown with vines and surrounded by towering trees, where stone statues of forgotten gods stand guard at the entrance, and sunlight filters through the thick canopy above, casting dappled shadows on the moss-covered stones that make up the temple's walls and steps.

Figure 9: Text-to-Image Generation results.

As can be seen, the win ratios are 89% for the SDXL + TULIP model and 11% for the SDXL + CLIP model, reflecting the enhanced alignment capability that we observe in the qualitative comparisons as well. The following instructions were provided to the annotators:

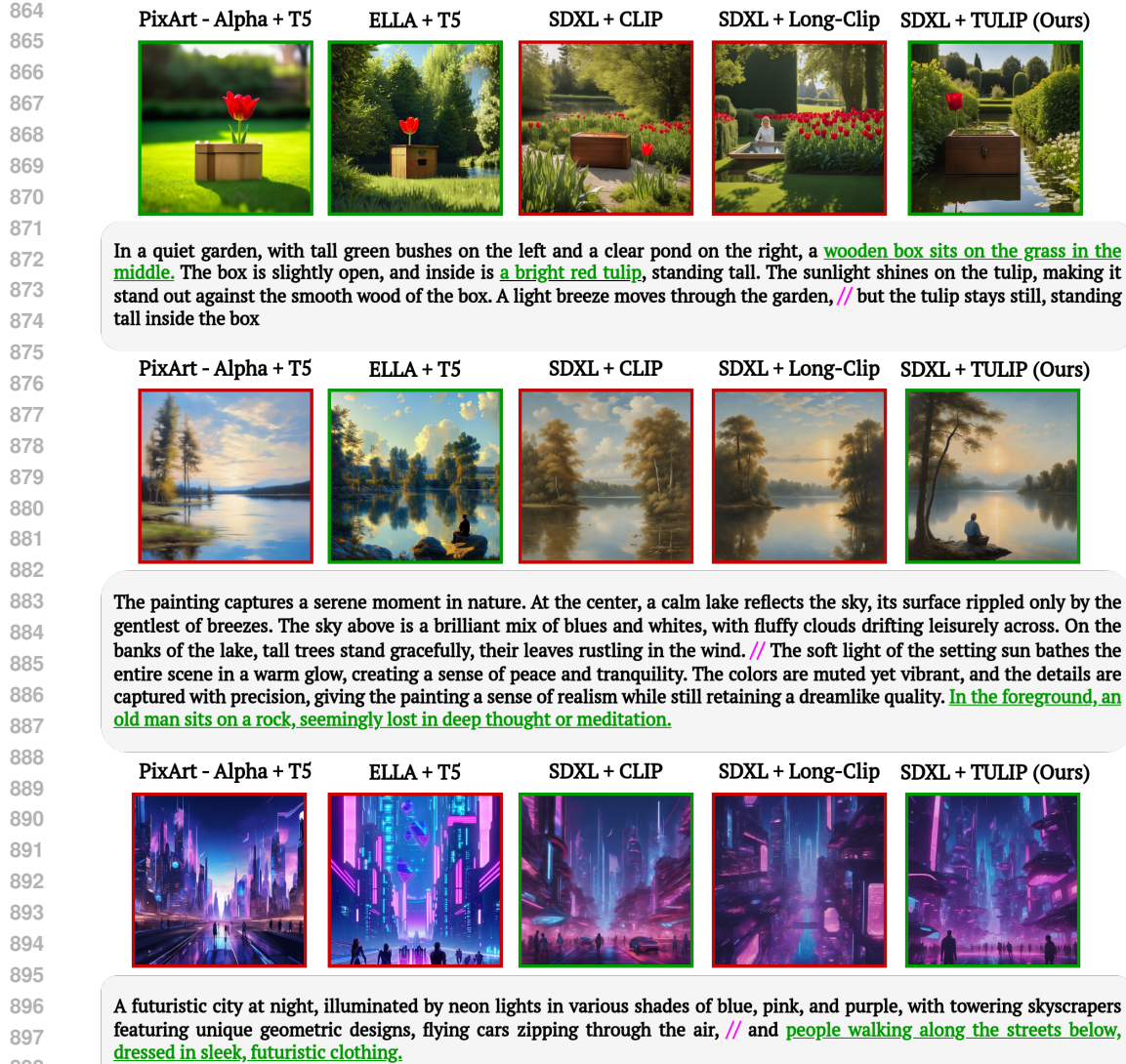


Figure 10: **Qualitative comparison of image generation models based on T5 (PIXART-Alpha and ELLA), CLIP, Long-CLIP, and TULIP.** Our TULIP-based model demonstrates the ability to generate images with nuanced details from captions, offering a plug-and-play solution without requiring costly retraining.

Instructions for annotators:

You are provided with 20 samples, each containing a prompt and two images generated by two different Stable Diffusion models. Your task is to compare the two images given the input prompt and choose the one you find more aligned with the prompt. Note that the differences might be very nuanced in some cases. Pay attention to the object attributes, relationships, verbs, object counting, etc.

A.3 COMPARISON BETWEEN TULIP AND T5-BASED MODELS

T5 text encoder (Roberts et al., 2019) is well-known for handling of long captions. We provided a qualitative comparison between our TULIP-based model and two T5-based models, PIXART-Alpha (Chen et al., 2023a) and ELLA (Hu et al., 2024), as shown in Figure 10, 11 and 15-20 of the Appendix. The comparison demonstrates that all models perform on par in generating high-



Figure 11: **Qualitative comparison of image generation models T5, CLIP, Long-CLIP, and TULIP.** Our TULIP-based model demonstrates the ability to generate images with nuanced details from captions, offering a plug-and-play solution without requiring costly retraining.

Method	Win rate (%)
SDXL + CLIP	11
SDXL + TULIP (Ours)	89

Table 5: **Human evaluation results.** The results are reflecting the enhanced alignment capability that we observe in the qualitative comparisons as well.

quality images from long and nuanced text descriptions. However, our TULIP approach stands out due to its plug-and-play capability for image generation, requiring no additional fine-tuning. This characteristic makes TULIP more versatile and practical compared to the fine-tuning demands of the T5-based counterparts.

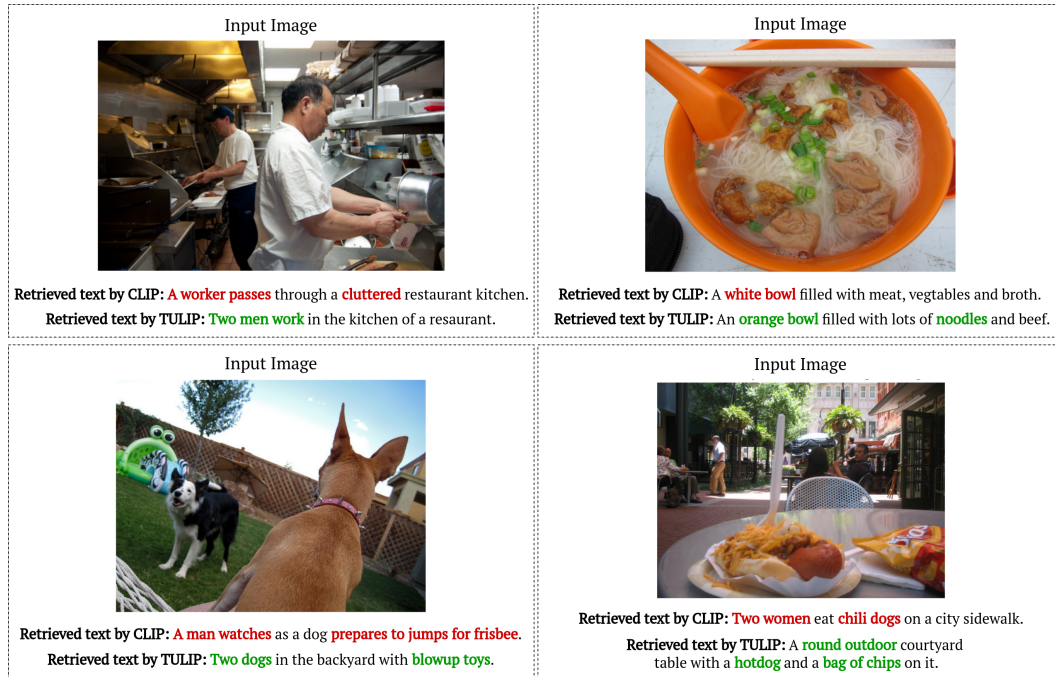


Figure 12: **Qualitative comparison of image-to-text cross-modal retrieval between CLIP and TULIP.** We can observe that our TULIP model can capture the fine-grained details in both captions and images. Note that the red text color indicates visually misclassified concepts in the images, whereas the green color indicates correct ones.



Figure 13: **Qualitative comparison of text-to-image cross-modal retrieval between CLIP and TULIP.** We can observe that our TULIP model can capture the fine-grained details in both captions and images. Note that the red text color indicates visually misclassified concepts in the images, whereas the green color indicates correct ones.

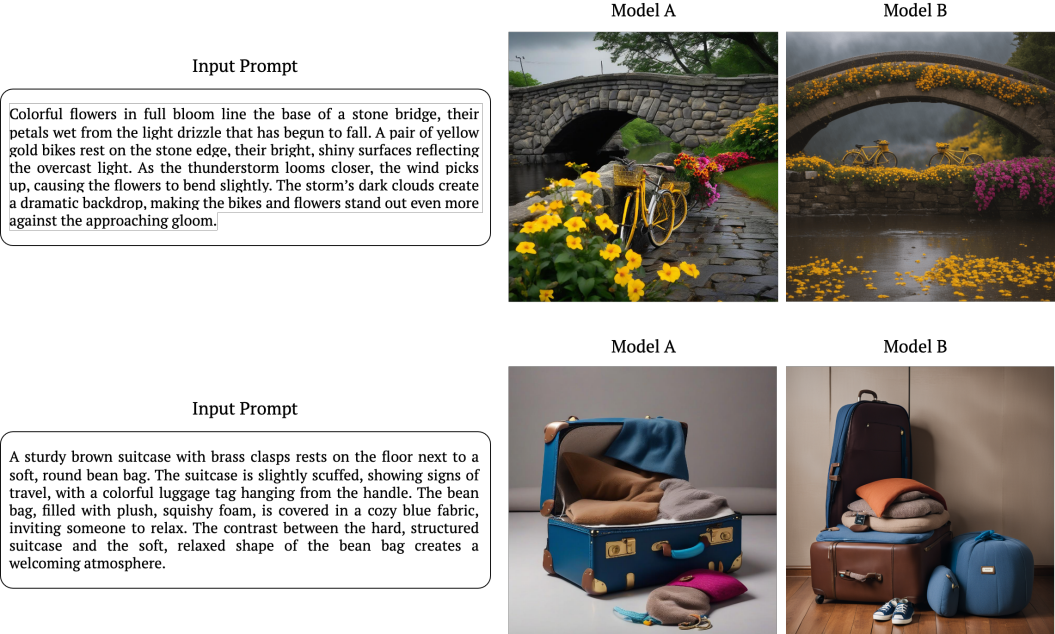


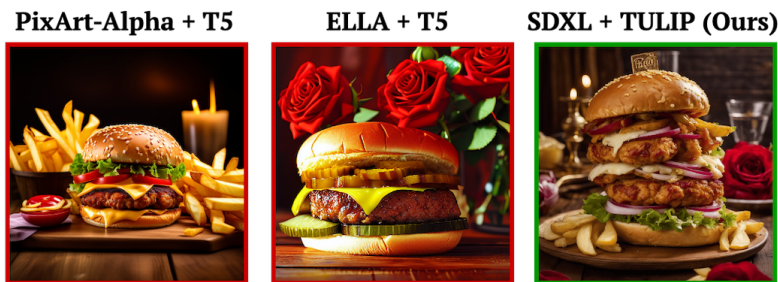
Figure 14: Example of a sample in the human evaluation. We provide the text prompt and two randomized images generated by SDXL.



Two tall white Christmas trees, adorned with twinkling lights and colorful ornaments, stand in the corner of a cozy living room. Beneath the trees, wrapped presents in shiny blue and golden paper and colorful ribbons are stacked in a small mountain.



Colorful flowers in full bloom line the base of a stone bridge, their petals wet from the light drizzle that has begun to fall. A pair of yellow gold bikes rest on the stone edge, their bright, shiny surfaces reflecting the overcast light. As the thunderstorm looms closer, the wind picks up, causing the flowers to bend slightly. The storm's dark clouds create a dramatic backdrop, making the bikes and flowers stand out even more against the approaching gloom.



A juicy double chicken burger, piled high with pickles, onions, and a perfectly cooked patty, is placed on a wooden table, the bun soft and golden. A pile of fries, crispy on the outside and fluffy on the inside, sits beside the burger, their golden color shining in the light. A bunch of red roses, their petals open and lush, sits in the background, adding a touch of elegance to the scene. The warm, inviting colors of the food contrast beautifully with the deep red of the roses.

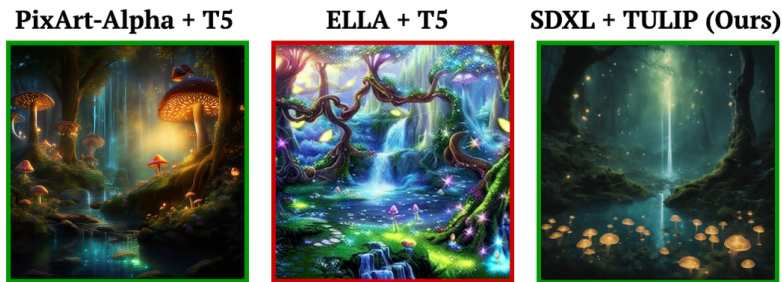
Figure 15: Comparison to T5-based models (PIXART-Alpha (Chen et al., 2023a) and ELLA (Hu et al., 2024)) for image generation.



A tall martini glass with a sleek, clear stem holds a perfectly mixed drink, the glass gleaming under the soft light. Inside the glass, a single green olive floats at the base, its shiny surface reflecting the light. Nearby, a plate of fresh oysters is arranged neatly, their glossy, wet shells slightly open, revealing the tender meat inside. The contrast between the elegant martini and the rustic oysters creates a striking visual pairing on the table.



A sturdy brown suitcase with brass clasps rests on the floor next to a soft, round bean bag. The suitcase is slightly scuffed, showing signs of travel, with a colorful luggage tag hanging from the handle. The bean bag, filled with plush, squishy foam, is covered in a cozy blue fabric, inviting someone to relax. The contrast between the hard, structured suitcase and the soft, relaxed shape of the bean bag creates a welcoming atmosphere.



An enchanted forest at dawn, where glowing mushrooms light up the forest floor, trees with twisted trunks and sparkling leaves reach towards the sky, and magical creatures like fairies and wisps float through the air, while a waterfall cascades into a crystal-clear pond in the background.

Figure 16: Comparison to T5-based models (PIXART-Alpha (Chen et al., 2023a) and ELLA (Hu et al., 2024)) for image generation.

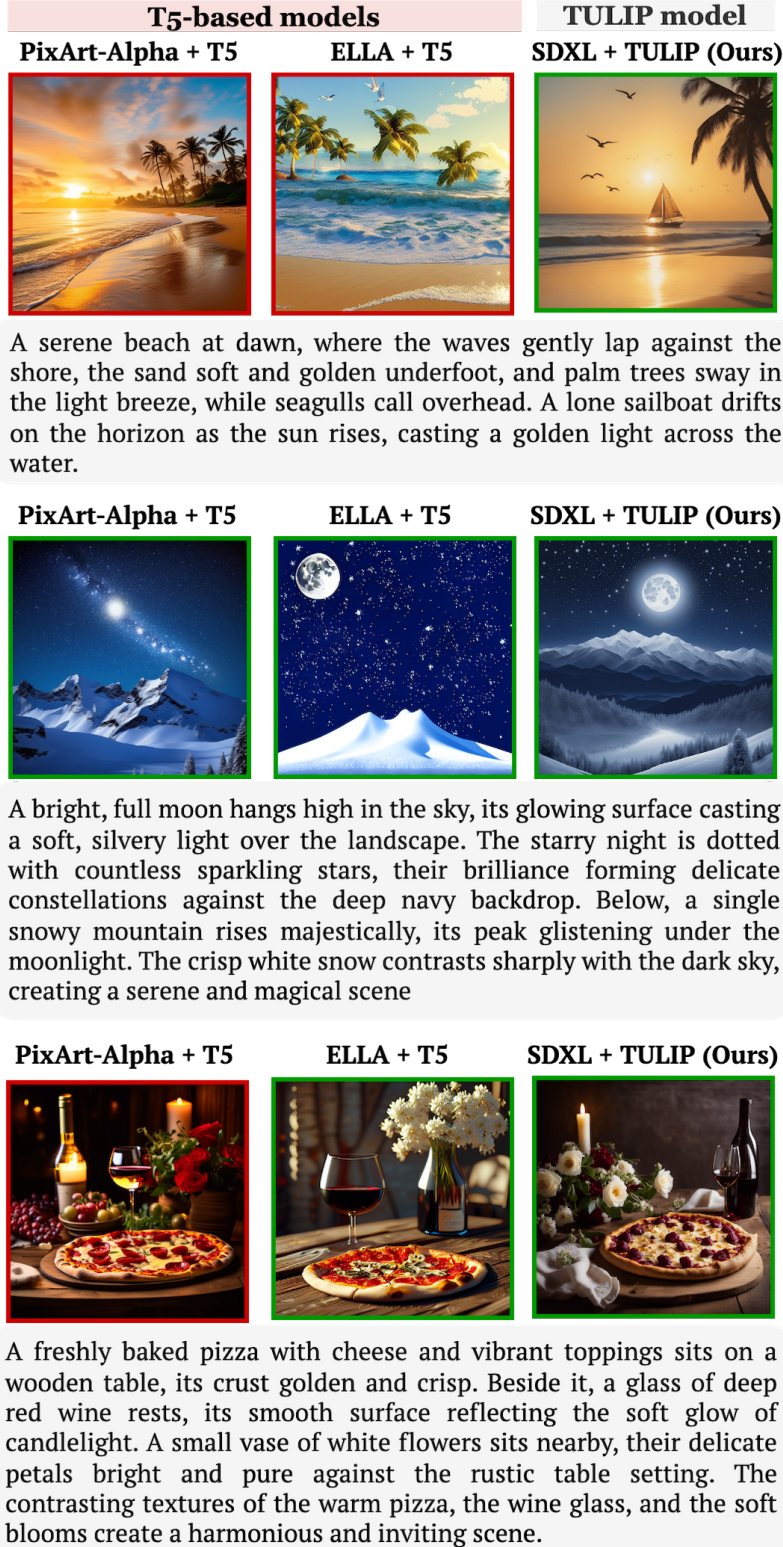
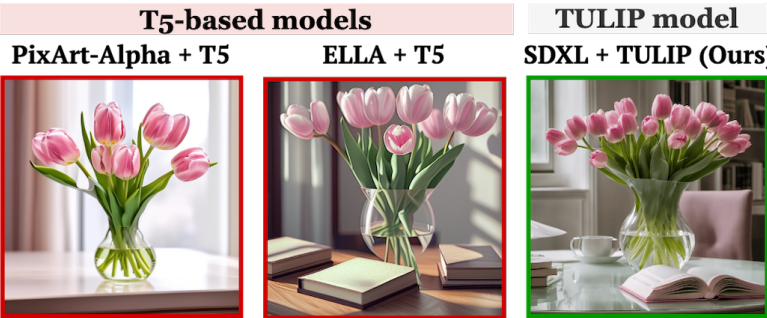


Figure 17: Comparison to T5-based models (PIXART-Alpha (Chen et al., 2023a) and ELLA (Hu et al., 2024)) for image generation.



A glass vase filled with fresh pink tulips sits in the center of a desk, the long green stems visible through the crystal-clear surface. The petals of the tulips are soft, their delicate pink hue adding warmth to the room. Next to the vase, a pair of neatly stacked books lies with one slightly ajar, revealing a glimpse of printed pages. The arrangement of flowers and books creates a serene, cozy corner ideal for reading or reflection.

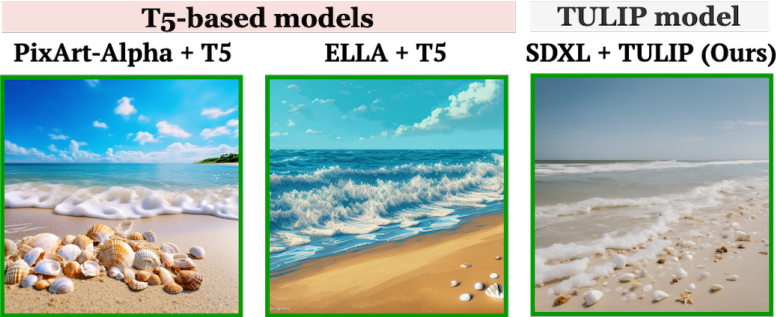


The purple cat lounges lazily on a sunny windowsill, its bright fur standing out against the light-colored wood. Its oversized sunglasses reflect the sunlight, adding a cool, fashionable touch to its relaxed pose.



The pink tiger stands gracefully in the corner of the house with a green sun glasses, and its vibrant fur shimmering in the sunlight streaming through the window. Its intense gaze blends with the calm atmosphere of the room, surrounded by plants and cozy furniture.

Figure 18: Comparison to T5-based models (PIXART-Alpha (Chen et al., 2023a) and ELLA (Hu et al., 2024)) for image generation.



A golden sandy beach stretches out under a blue sky, with gentle waves lapping at the shore. A few white seashells are scattered along the edge.



A birthday cake with creamy white frosting is decorated with blue and purple sprinkles and topped with lit candles. The cake sits on a table surrounded by white flowers next to a white dog.



A butterfly with orange and black wings flies gently over a vibrant flower field. The field is filled with colorful blooms of yellow and pink, their petals swaying in the breeze.

Figure 19: Comparison to T5-based models (PIXART-Alpha (Chen et al., 2023a) and ELLA (Hu et al., 2024)) for image generation.



Figure 20: Comparison to T5-based models (PIXART-Alpha (Chen et al., 2023a) and ELLA (Hu et al., 2024)) for image generation.